

# ON-BOARD DEPLOYMENT EVENT VERIFICATION FOR GOES-R SPACECRAFT

**Jim Chapel<sup>(1)</sup>, Timothy Bevacqua<sup>(2)</sup>, Graeme Ramsey<sup>(2)</sup>, Russell Gehling<sup>(3)</sup>,  
Timothy Rood<sup>(4)</sup>, Douglas Freesland<sup>(5)</sup>, Alexander Krimchansky<sup>(6)</sup>**

<sup>(1)</sup>*Lockheed Martin Space, Littleton, CO USA, +1-303-977-9462, [jim.d.chapel@lmco.com](mailto:jim.d.chapel@lmco.com)*

<sup>(2)</sup>*Lockheed Martin Space, Littleton, CO USA*

<sup>(3)</sup>*All Points Logistics, Merritt Island, FL, USA*

<sup>(4)</sup>*Advanced Solutions, Inc., Littleton, CO, USA*

<sup>(5)</sup>*The ACS Engineering Corporation, Clarksville, MD, USA*

<sup>(6)</sup>*NASA Goddard Space Flight Center, Greenbelt MD, USA*

## ABSTRACT

As is common with many spacecraft designs, the GOES-R vehicles require a series of deployment events to transition from the launch configuration to the operational configuration. Rather than implementing additional sensors to verify various deployments, the GOES-R program developed an alternate approach that uses existing gyro rate sensing. The approach includes two pieces: the first is a new onboard shock detection capability to confirm initiation of individual deployment events, and the second is a ground-based dynamics verification step to confirm completion of deployment events. We first present the algorithm that detects shock events for various deployment devices along with the parameter tuning performed during ground tests. We then show inflight performance of the shock detection algorithm. While shock detection is useful for observing initiation of deployment events, completion of some deployment events cannot be determined by shock detection alone. For these events, such as solar panel latch-up and deployable boom extension, the program developed dynamics models for the deployment transient responses. High-rate gyro data were recorded for these events, which allow the ground team to verify that the appendages were fully deployed. We show the predictive models for these events and corresponding flight results.

## 1 INTRODUCTION

The Geostationary Operational Environmental Satellite-R program (GOES-R) now has three fully operational next-generation weather satellites on orbit. GOES-16 launched in November 2016, GOES-17 launched in March 2018, and GOES-18 launched in March 2022. The GOES-R series of spacecraft provide dramatic improvements in geostationary orbit (GEO) weather observation capabilities over the previous generation [1]. The overall GOES-R spacecraft configuration is shown in Figure 1 and includes both Earth-observing and Sun-observing instruments.

For the GOES-R spacecraft, many of the deployment events occur during periods where downlink capability is very limited. Furthermore, many of these deployments need to be completed successfully before proceeding to the next activity—executing subsequent steps could be potentially catastrophic if the preceding steps were not successfully accomplished. For GOES-R spacecraft, there are 9 separate deployment events needed to transition to the operational configuration. These events include solar array deployments, antenna deployments, Earth-Pointed Platform (EPP) launch lock release, and other instrument related deployments. There are four different types of release devices, including separation nuts, frangibolts, Split Spool Release Devices (SSRDs), and launch lock devices. In total, there are 28 device firings to be detected across all the deployment events. Each device exhibits a different signature as seen by the gyros depending upon the device type, the orientation of the device, and the location of the device relative to the gyros. Sensors could be employed to detect

specific deployment events, but this would require significant additional spacecraft resources, and some types of deployment events may require complex sensor implementations to reliably detect them. In this paper, we present two simple and reliable approaches developed by the GOES-R program for verifying various deployment events.

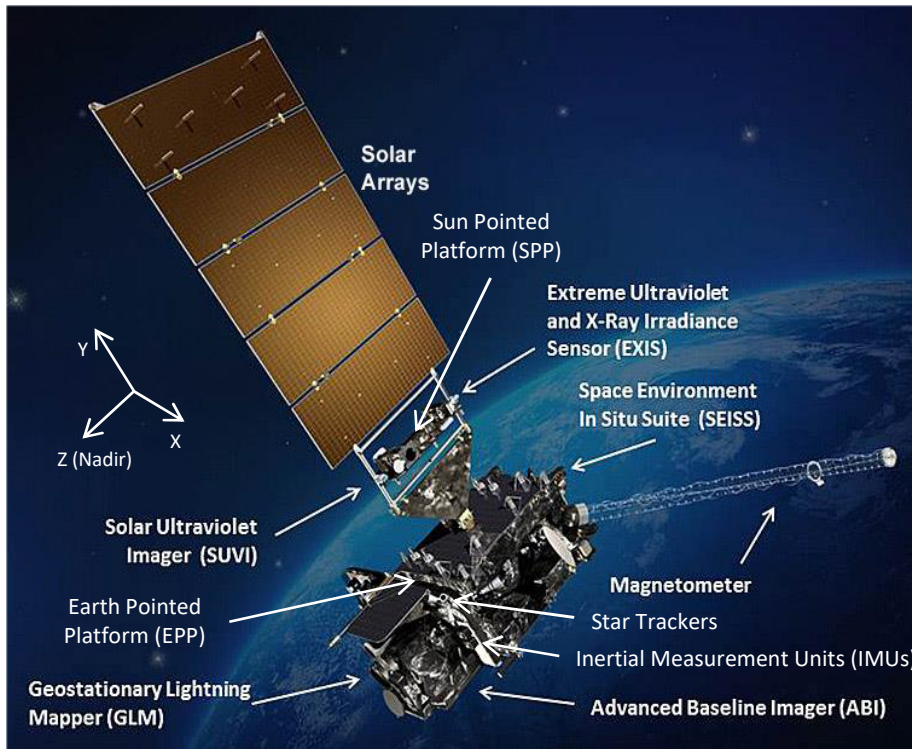


Figure 1. GOES-R Spacecraft in Operational Configuration

The first of these approaches utilizes 200 Hz gyro data to detect shock events, which occur at the initiation of each deployment activity. The onboard shock detection algorithm is specifically designed to report the results using minimal telemetry resources. The second approach is a ground-based technique that compares the 200 Hz gyro data signature with the predicted dynamic response for completion of a specific deployment event. The high-rate gyro data is recorded onboard for a limited period of time and downlinked using low-bandwidth telemetry. Once the deployment has been confirmed by the ground, the Operations Team can then proceed with subsequent activities. The subsequent sections will describe the GOES-R shock detection algorithm, the derivation of the algorithm parameters from ground test data, shock detection flight results, the development of deployment models for the solar array and magnetometer boom deployments, and flight results for those deployments.

## 2 SHOCK DETECTION ALGORITHM AND PARAMETER DEFINITION

As input, the shock detection algorithm processes 200 Hz gyro delta angles to determine whether a shock event has occurred. The algorithm runs at 20 Hz but operates on 200 Hz delta angles from the 4-gyro Inertial Measurement Unit (IMU) [2][3][4]. At 20 Hz, the algorithm computes cumulative angular motion over rolling 0.01 second windows per gyro, computes the mean and standard deviation statistics on the 200 Hz cumulative angles, and compares the statistics to a threshold. A shock counter is incremented whenever the 20 Hz statistic for more than 1 gyro is above the threshold. An event counter increments when the shock counter first increments, after not incrementing for some configurable number of previous cycles. A single command is used to enable or disable the algorithm. The enable command sets 3 configurable parameters and clears previous shock and event counters.

When enabled, the algorithm will compute the statistics on the angular motion measured by each gyro and counts the number of gyros for which the angular motion exceeds a threshold. However, the

algorithm will not declare shock events unless high-rate gyro data is being recorded—high-rate gyro data is recorded for some short period of time for every deployment event. This allows the ground to trend the background 20 Hz statistics in a quiescent state prior to the actual deployment activity.

It should be noted that this algorithm operates on raw, unfiltered gyro delta angles, and does not compensate for gyro biases estimated by the attitude Kalman filter. Large gyro biases could make the shock event detection less robust. However, the algorithm has been extensively tested on gyro data recorded during ground testing, which include uncompensated earth rates. Earth rates are many times larger than the maximum expected gyro bias. Ground test data are used to determine the three configurable parameters used by the algorithm, which are shown in Table 1. Each deployment event has a unique signature as seen by the gyros, so the parameters are different from one deployment event to another. Setting the detection threshold too high will result in missed events. Setting the detection threshold too low will result in false shock detections.

Table 1. Shock Detection Algorithm Parameters

Parameter	Description
Detection Threshold	This sets the gyro delta-angle detection threshold ( $\text{mean} + N * \text{sigma}$ ) for the next rolling window
Minimum Cycles Between Events	Sets minimum 20 Hz cycles between shock event detections
Sigma Multiplier	Sets the standard deviation multiplier, N
Enable/Disable	Sets the enable state of the algorithm

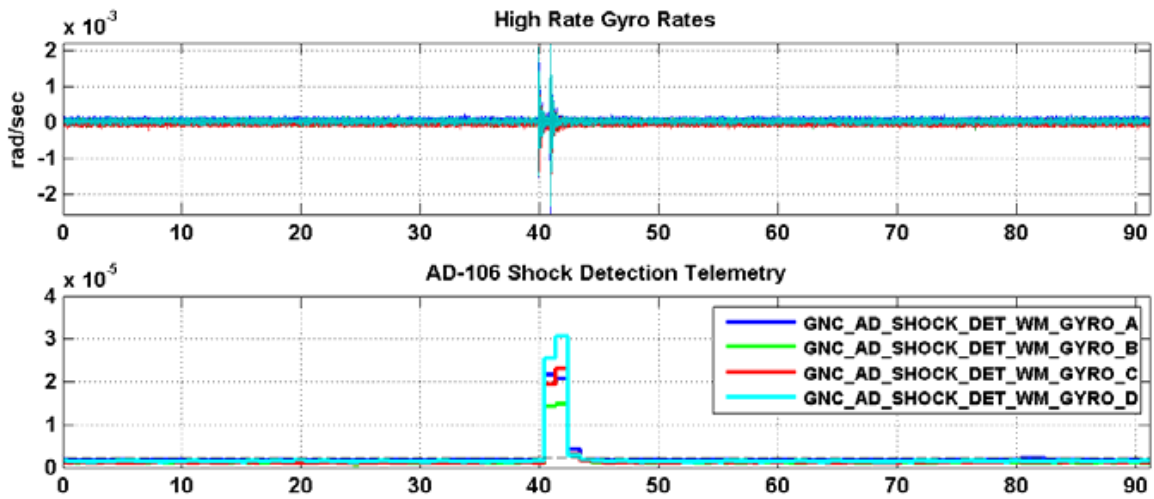
## 2.1 Initial Shock Detection Testing, Pre-GOES-16 Launch

As mentioned above, gyro data collected during ground test will always include earth rate, whereas the actual deployments in flight are performed in a quiescent, non-rotating state. Based upon analysis and simulation, the shock detection algorithm performance was shown to be insensitive to this difference between ground test and flight. To verify the functionality of the algorithm, unit test data were generated from unaltered ground test data, and the results were used and to derive an initial set of parameters. Although the algorithm was determined to be insensitive to earth rates, it was quickly discovered that technician activity around the spacecraft seriously degraded the shock detection performance. Activity constraints were placed on the test team, which prevented false detections during ground test and allowed determination of the shock detection parameters for flight.

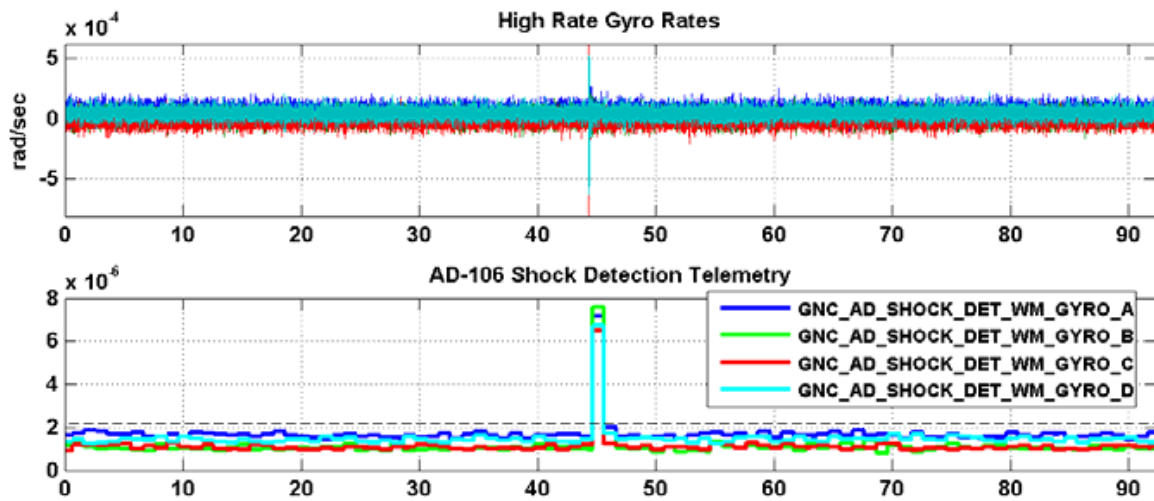
Test case data were created from high-rate gyro data collected during various GOES-16 ground deployment tests. These tests included solar array, antenna wing, x-band reflector, Earth-pointed platform, and magnetometer boom deployments. Collection of this data allowed off-line simulation of on-orbit deployment events and the derivation of the shock detection parameters for flight. Examples of the ground test data are presented below.

The most involved deployment activity involves the “second stage” deployment of the solar array, which results in the configuration shown in Figure 1. The “first stage” of the solar array deployment occurs autonomously shortly after separation from the launch vehicle, and allows full power collection from the five solar panels. However, the Sun Pointed Platform (SPP) is still stowed in the first stage configuration, and the two gimbals controlling the solar array and the SPP orientations are locked. Only after the second stage deployment are the solar array and SPP in a fully operational configuration.

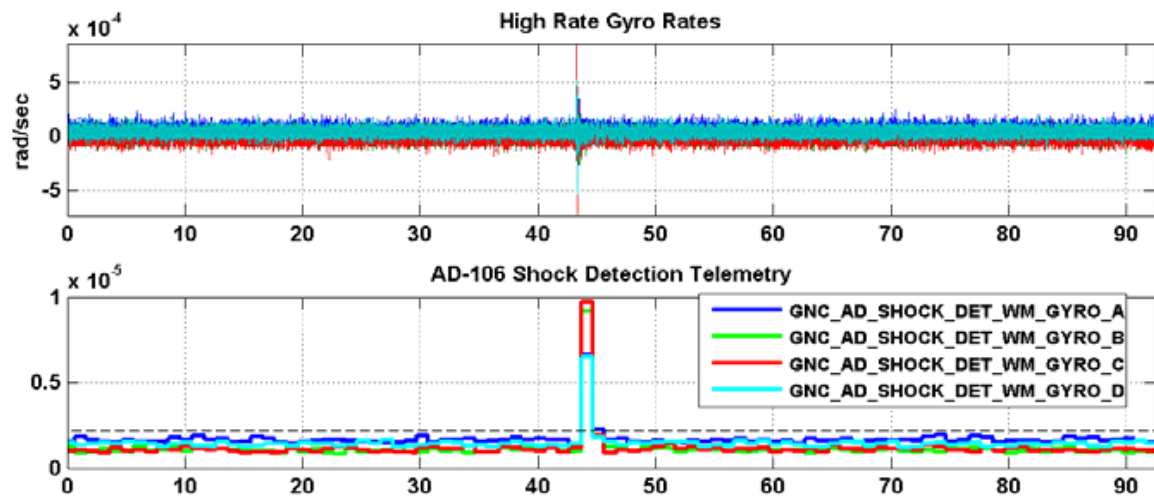
The deployment comprises sequential firing of 4 frangibolts, and the activation of 6 Split Spool Release Devices (SSRDs). It is critical that the frangibolts be fired prior to activation of the SSRDs to achieve a successful deployment. The high-rate gyro data collected during ground testing for these 10 events are shown in Figures 2 and 3 for the frangibolts and SSRDs respectively. Also shown are the raw shock detection data for each event.



a) First Two Frangibolts, Solar Array (Step 1)



b) Third Frangibolt, Solar Array Yoke (Step 2)



c) Fourth Frangibolt, Solar Array Yoke (Step 3)

Figure 2. Ground Test Gyro Rate and Shock Detection Data for Solar Array Deployment

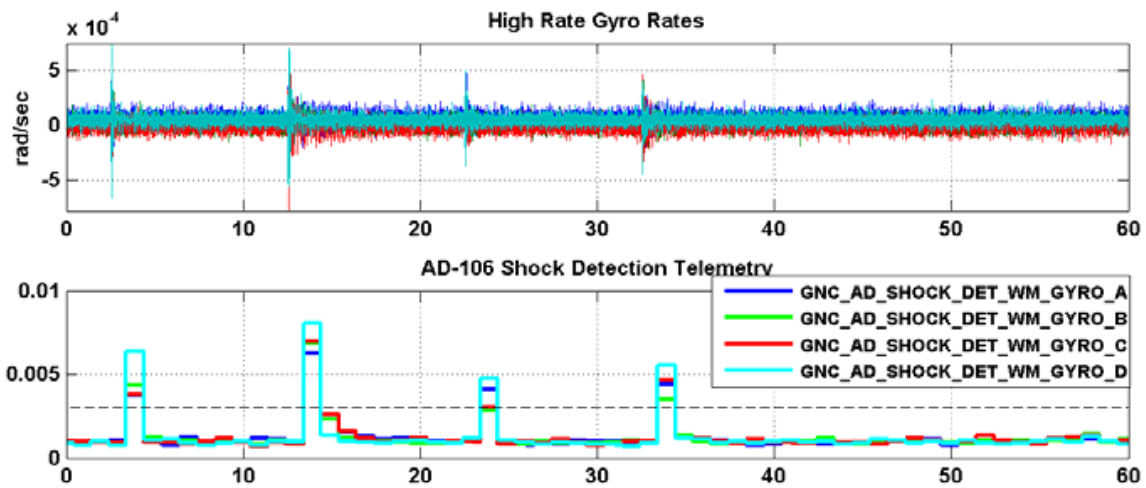


Figure 3. Ground Test Gyro Rate and Shock Detection Data for SPP Deployment (Steps 4 and 5)

As can be seen from the above plots, there is significant signature variability among the various shock events, even for the same type of release device. However, the deployment events for the solar array and SPP are clearly visible in the high-rate gyro data, so the algorithm parameters can be tuned to reliably detect the shock events.

Most of the deployment events involve simple, direct load paths from the shock source to the IMU mounting location, which results in a clear response as seen by the gyros. Another example of a strong shock signature can be seen in the EPP deployment of the four launch lock mechanisms, which are also SSRD devices. This is expected because the IMU is mounted on the EPP. The EPP deployment is much more difficult to test on the ground, as the entire EPP must be offloaded for the test [5][6]. The test was performed successfully, and the resulting GOES-16 ground test data for the EPP deployment is shown in Figure 4.

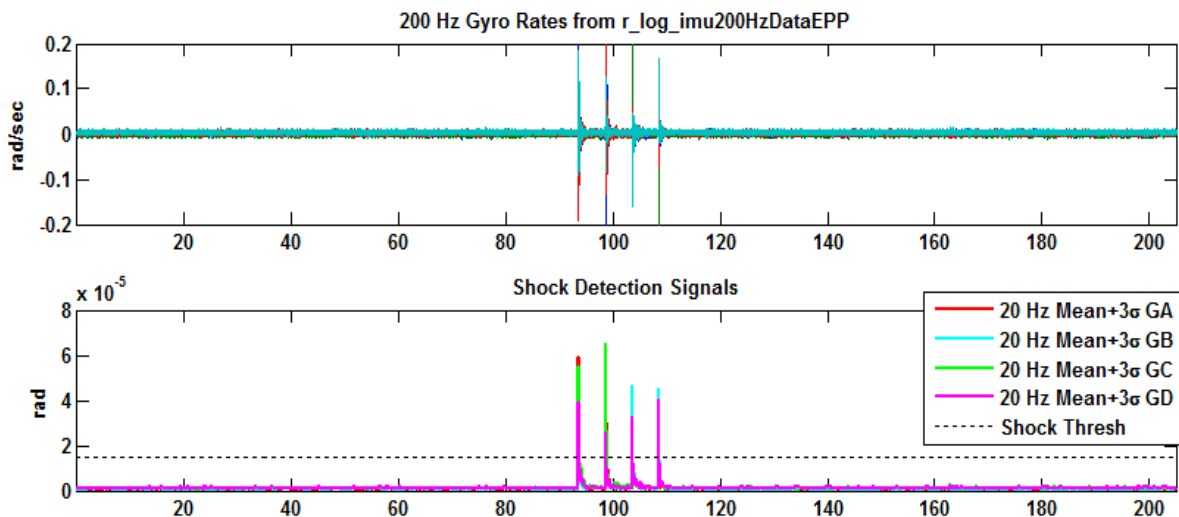


Figure 4. Ground Test Gyro Rate and Shock Detection Data for EPP Deployment

Comparison of gyro data for the EPP deployment in Figure 4 and the SPP deployment in Figure 3 shows that the gyro signature is  $\sim 300X$  larger for the EPP deployment. This is due to the close proximity of the IMU to the launch locks, and the direct load path from the launch locks to the IMU.

The MAG instrument boom deployment is an example of a shock event that has relatively low observability from the IMU. That deployment only uses a single frangibolt, and the frangibolt is located on the -Z base panel of the vehicle nearly as far away from the IMU as possible. The ground

test data for the GOES-16 MAG boom deployment is shown in Figure 5. Even with the large distance between the frangibolt and the IMU, the shock event is clearly visible in the gyro data.

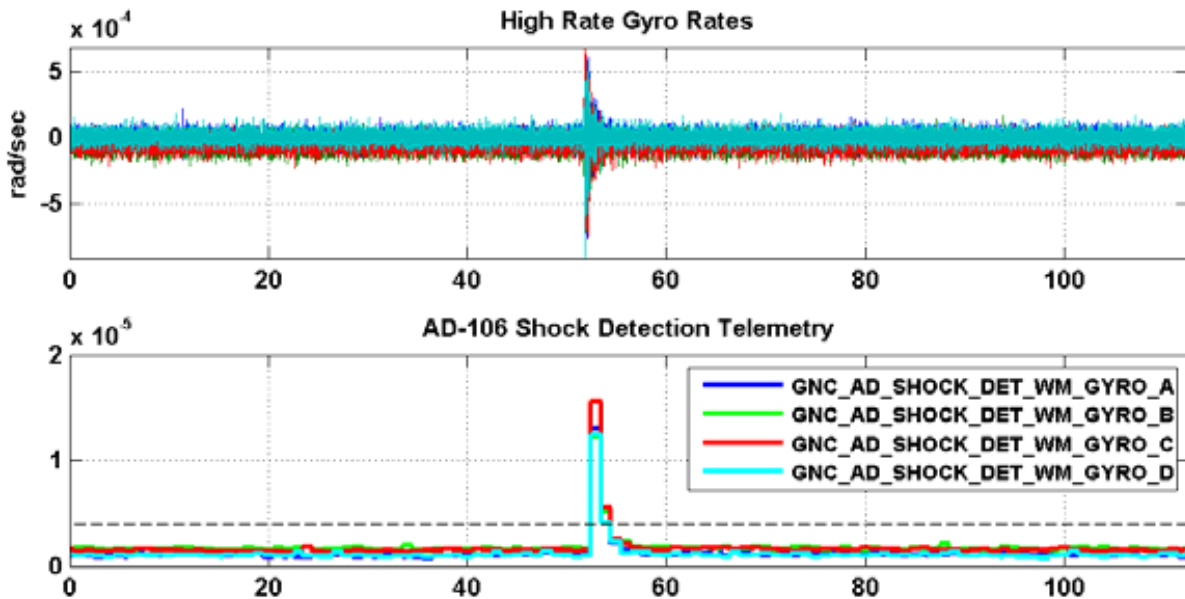


Figure 5. Ground Test Gyro Rate and Shock Detection Data for MAG Boom Deployment

## 2.2 Shock Detection Parameter Definition for GOES-16, GOES-17 and GOES-18

Ground deployment test data presented above were used to seed the shock detection simulation, and the resulting parameters for GOES-16 are shown in Table 2 for the various deployments. Flight results from GOES-16 were subsequently used to tune the parameters for GOES-17 and GOES-18, which are also shown in Table 2. Most of the deployment events were adequately captured from the ground testing, but several events required additional parameter tuning for GOES-17 and GOES-18. Updates from the initial parameter settings used on GOES-16 are shown in blue. Shock events from frangibolt firings and SSRD activations were always detected using the initial parameter set derived from ground test data. However, in two cases more shock events were observed in telemetry than expected. The flight results and subsequent parameter tuning will be discussed in more detail in the next section, The on-orbit ABI door release deployment shown in Table 2 had high rate IMU data recorded in-flight for GOES-16, but no prelaunch shock detection parameters had been developed. The flight data was used to generate vehicle shock detection parameters for subsequent vehicles.

Table 2. Shock Detection Parameterization Results from Simulation, used on GOES-16/17/18

	Detection Threshold (mean +N*sigma)	Minimum Cycles Between Events	Sigma Multiplier (N)
Solar Array Step 1 (Frangibolt, 2X)	<b>2.2e-6</b> / <b>0.01</b> / 0.01	<b>10</b> / 10 / 10	3 / <b>3000</b> / 3000
Solar Array Step 2 (Frangibolt, 1X)	<b>2.2e-6</b> / 2.2e-6 / 2.2e-6	<b>10</b> / 10 / 10	3 / 3 / 3
Solar Array Step 3 (Frangibolt, 1X)	<b>2.2e-6</b> / 2.2e-6 / 2.2e-6	<b>10</b> / 10 / 10	3 / 3 / 3
Solar Array Step 4 (SSRD, 4X)	<b>0.003</b> / 0.003 / 0.003	<b>40</b> / 40 / 40	3000 / 3000 / 3000
Solar Array Step 5 (SSRD, 2X)	<b>0.003</b> / 0.003 / 0.003	<b>40</b> / 40 / 40	3000 / 3000 / 3000
Antenna Wing (Frangibolt, 4X)	<b>0.005</b> / 0.005 / <b>0.003</b>	<b>20</b> / 20 / 20	3000 / 3000 / 3000
X-band Reflector (Frangibolt, 3X)	<b>4.0e-6</b> / 4.0e-6 / 4.0e-6	<b>10</b> / 10 / 10	3 / 3 / 3
Earth-Pointed Platform Launch Locks (SSRD, 4X)	<b>1.5e-5</b> / 1.5e-5 / 1.5e-5	<b>10</b> / 10 / 10	3 / 3 / 3
MAG Boom (Frangibolt, 1X)	<b>4.0e-6</b> / <b>0.015</b> / <b>0.01</b>	<b>10</b> / <b>50</b> / 50	3 / <b>3000</b> / 3000
Advanced Baseline Imager Door Opening*	N/A / <b>4.0e-6</b> / <b>5.0e-5</b>	N/A / <b>40</b> / 40	N/A / <b>3</b> / 3

\* Determined during GOES-16 on-orbit deployment, not ground test

### 3 SHOCK DETECTION RESULTS, SIMULATION VS. FLIGHT

This section presents shock detection simulation results using ground test data and compares those results to those observed in flight. The same parameters shown in Table 2 were used in the simulations and the flight operations. The shock detection algorithm successfully identified the correct number of release events for all but two of the GOES-16 on-orbit deployments: Step 1 of the solar array deployment and the MAG boom deployment. In both of those deployments the algorithm successfully detected the initial shock event in-flight, but then reported more events than expected. This result differed from the ground test results, where the expected 2 shocks were observed for the Solar Array Step 1, and the expected single shock was observed for the MAG boom deployment.

#### 3.1 Solar Array Deployment

Ground testing of the GOES-16 solar array deployment was performed using the shock detection parameters shown in Table 2. The solar array, boom, and yoke assemblies cannot support the weight of the large solar array in a 1-g environment, so an offload apparatus must be used for ground tests [5][6]. The deployment results are shown in Figure 6, with the shock detection algorithm performing as expected. The initial 2 frangibolt firings are detected followed by sequential firings of the remaining 2 frangibolts. Then 4 SSRDs are activated nearly simultaneously, followed by the remaining 2 SSRDs. The solar array is deployed from the bus once the final SSRDs are activated. The expected number of shock events are observed in the top plot of Figure 6, with a total of 10 events recorded at the end of the deployment sequence.

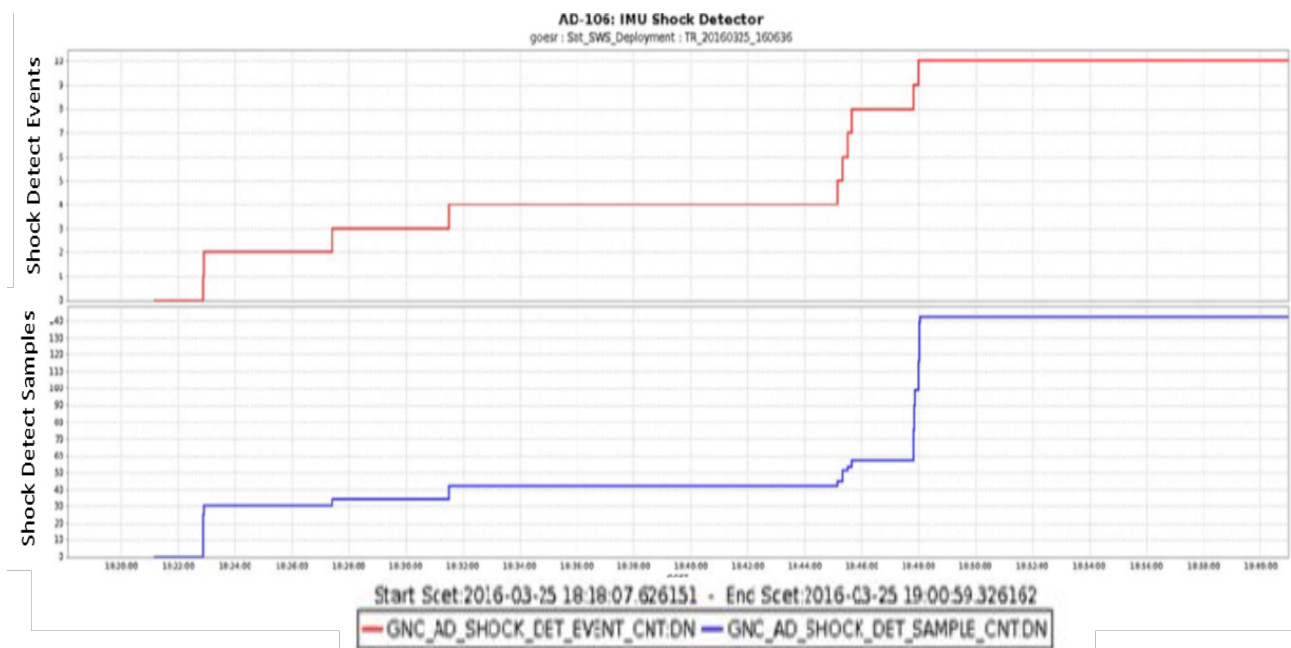


Figure 6. Ground Test Shock Detection Results for Solar Array Deployment

The shock detection response in flight for the solar array deployment exhibited some differences from ground test. Specifically, when the Step 1 frangibolts released there was a significant ringing in the gyro rate response that did not occur during ground test. Instead of the expected 2 shock events, the shock detection algorithm reported a total of 46 shock events. This is shown in Figure 7. Close examination of the gyro rate data shows the two frangibolt firings at around 40 seconds on the upper plot. The response magnitude was somewhat lower than observed in ground test, but it remains within the projected uncertainty. However, the ringing seen following the frangibolt firings was not expected and triggered additional “shock” events. Clearly, the parameters were not tuned to account for this ringing effect, and as shown in Table 2, the parameters were adjusted for subsequent vehicles to account for the ringing. Updated parameters were used on both GOES-17 and GOES-18. The shock detection results for GOES-18 are shown in Figure 8 with the expected 2 shock events clearly evident.

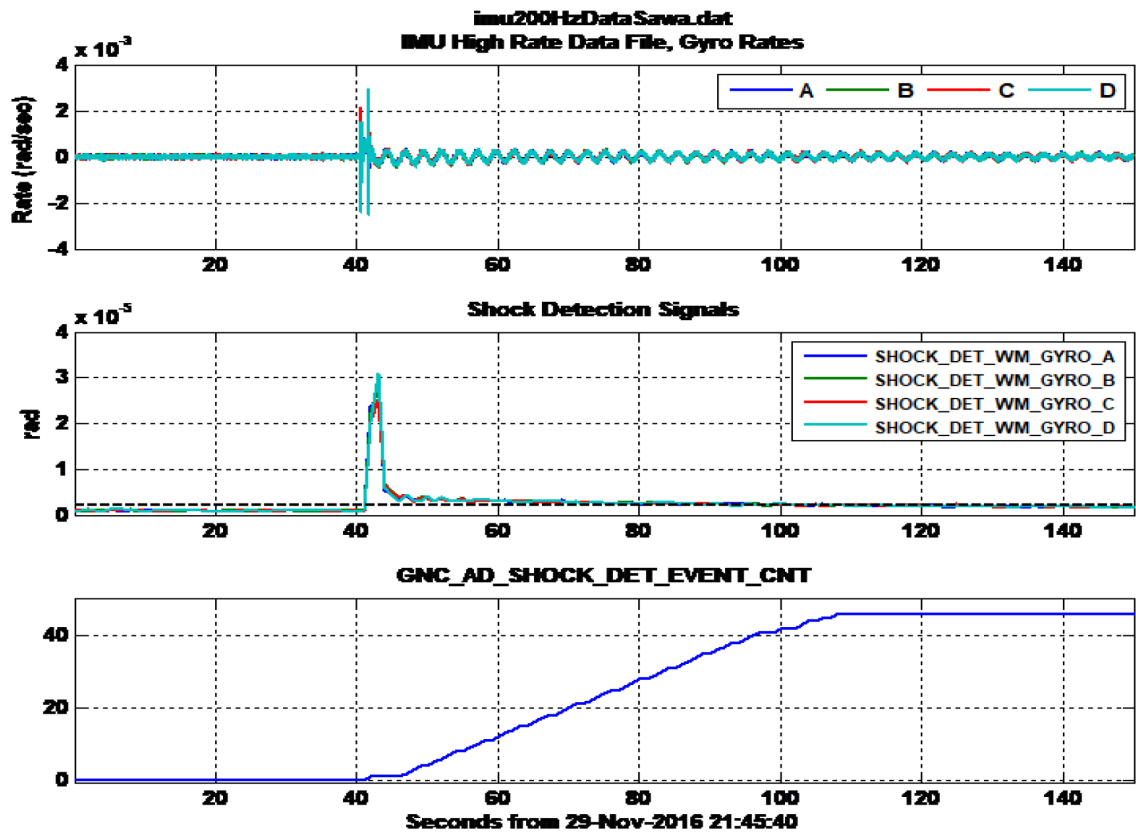


Figure 7. GOES-16 Flight Results of the Solar Array Deployment, Step 1

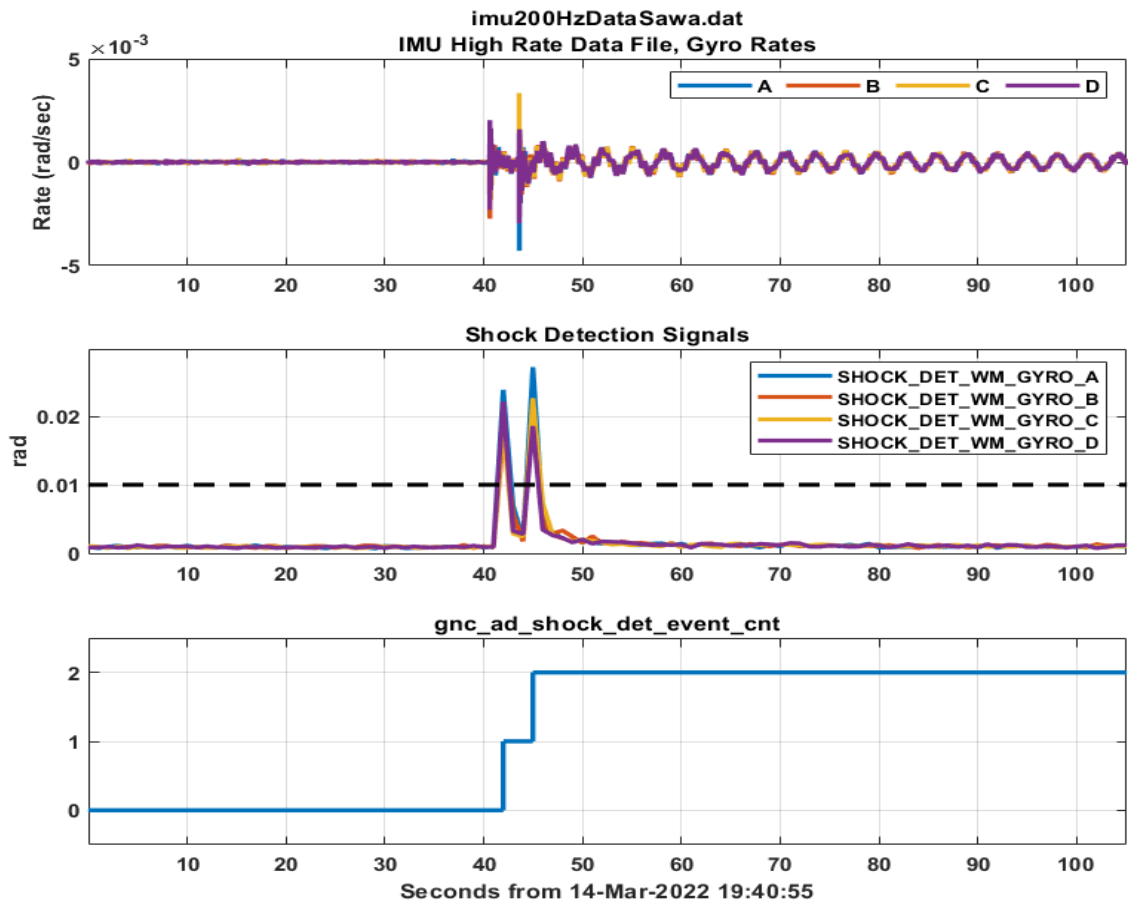


Figure 8. GOES-18 Flight Results of the Solar Array Deployment, Step 1

The other two frangibolt firings in Steps 2 and 3 also excited some ringing effects, but the response was less pronounced than the first two firings and the parameter selection worked as designed. No parameter adjustment was made for either Step 2 or Step 3, and the shock events were successfully detected on GOES-17. However, on GOES-18 the ringing did cause additional “shock” events to be detected, and the parameters for Step 2 and Step 3 are being reviewed for possible adjustment on GOES-19.

Step 4 of the solar array deployment sequence also showed some unexpected behavior, even though the shock detection itself performed nominally. This can be seen from the plots shown in Figure 9. As with the frangibolt firings, the SSRD activations induced a ringing response clearly evident in the gyro rate data. The 1<sup>st</sup>, 2<sup>nd</sup>, and 4<sup>th</sup> SSRD activations are apparent in the rate data, but the 3<sup>rd</sup> SSRD response is barely visible. This also shows up in the middle plot, where the detection is barely above the threshold for the 3<sup>rd</sup> SSRD, unlike the others which are significantly above the threshold. Fortunately, shock detection algorithm identified each of the events including the 3<sup>rd</sup> SSRD, although there was not much margin in detecting the 3<sup>rd</sup> SSRD activation. The ground tests performed prior to launch did not predict this behavior—all of the responses were reasonably close to each other in the ground test data, and all were well above the threshold. The same parameters were used for GOES-17 and GOES-18, and the performance was similar to ground test. Finally, the Step 5 shock detection worked as expected, and the observed SSRD signatures were in line with the ground test responses.

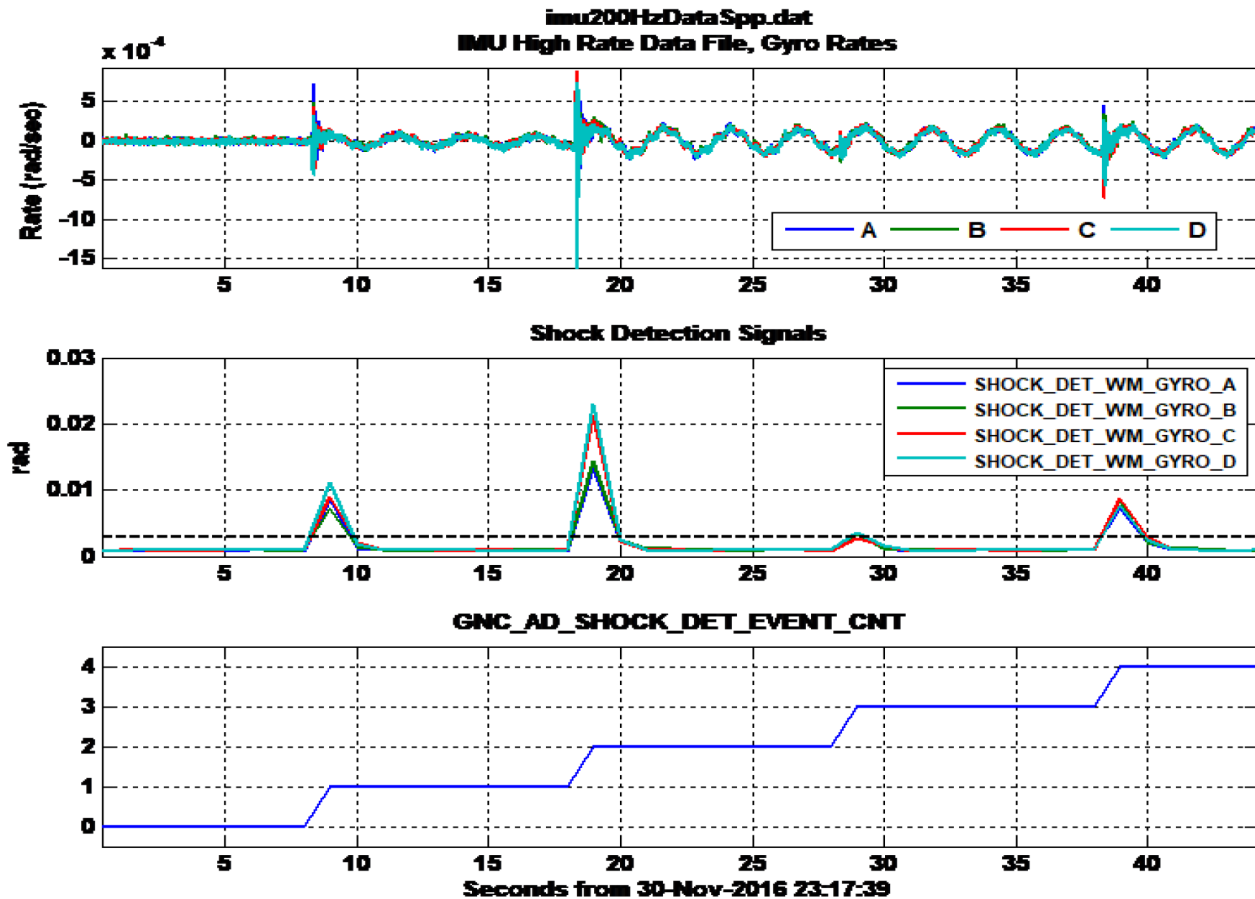


Figure 9. GOES-16 Flight Results of the Solar Array Deployment, Step 4

### 3.2 Earth Pointed Platform (EPP) Deploy

The EPP deployment consists of actuating 4 launch lock devices, which incorporate SSRDs in the mechanism design. As discussed above, the launch locks are located in close proximity to the IMU,

so their gyro rate signature is very strong. As expected, the shock detection algorithm worked flawlessly for this deployment on all three vehicles launched to date. The GOES-17 EPP deployment is shown in Figure 10. It is interesting to note that the activation signature of each launch lock becomes smaller as more launch locks are fired. The signatures are all well above the detection threshold, and the expected number of shock events are identified.

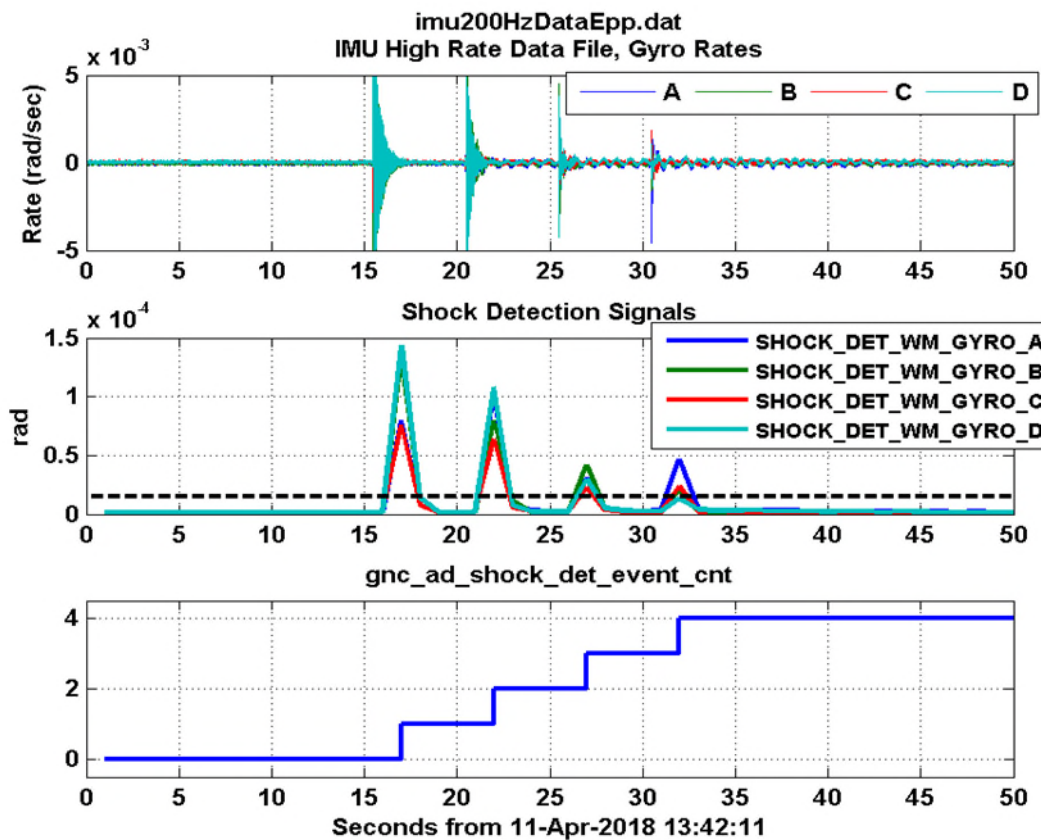


Figure 10. GOES-17 On-Orbit Shock Detection during EPP Deployment

### 3.3 GOES-18 Magnetometer Instrument (MAG) Boom Deployment Results

As discussed above, the MAG boom deployment utilizes a single frangibolt device to initiate the deployment sequence for the collapsible 8.5 m boom. The release device is located far away from the IMU, the sequence involves energetic dynamics as the boom extends, and the boom deployment cannot be fully tested at the spacecraft level. These factors make determination of appropriate shock detection parameters a challenge. As discussed earlier, the frangibolt firing in ground test provided a clear signature as seen by the gyros, and the resulting parameters are shown in Table 2. Not surprisingly the GOES-16 flight results were more complex, as shown in Figure 11. The frangibolt firing is clearly visible in the shock detection plot at around 25 s, but the shock is not appreciably larger than the boom deployment dynamics following the frangibolt firing. As the longerons snap into place, they produce a signature similar in magnitude to the frangibolt firing. When the boom locks into the deployed configuration at around 65 s, the gyro signature is higher than the frangibolt firing. The ringing of the boom in the deployed configuration continues to produce gyro rate magnitudes that are as large or larger than the response to the frangibolt firing. Instead of the single shock event expected from the shock detection algorithm, the results indicated 38 “shock” events using the parameters shown in Table 2.

The high-rate gyro data was downlinked from GOES-16, and parameter tuning was attempted for GOES-17, as reflected in Table 2. With the updated shock detection parameters, no events were detected for the GOES-17 MAG boom deployment at all because the shock detection signal did not exceed the specified threshold. Because the real-time telemetry show the boom deployment effects

on spacecraft body rates, the shock detection for this particular deployment event is not considered critical. Nonetheless, the high-rate telemetry from GOES-17 was used to create a new set of parameters for GOES-18. Unfortunately, no events were detected for the GOES-18 MAG boom deployment because the shock detection signal once again did not exceed the specified threshold. The onboard algorithm uses 200 Hz gyro telemetry in the computation of shock events, but the recorded telemetry only includes 100 Hz gyro telemetry for this deployment because of space limitations. This makes ground-based tuning of the shock detection parameters more difficult for the MAG boom deployment.

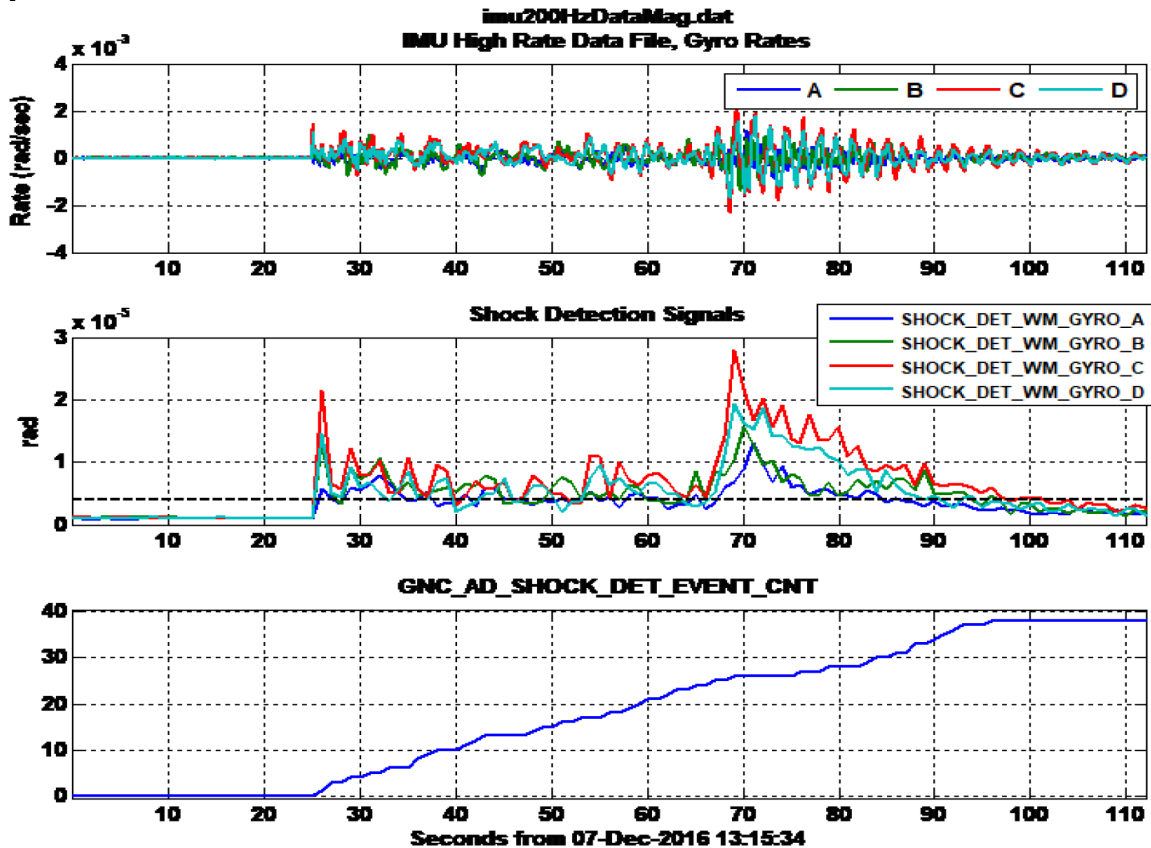


Figure 11. GOES-16 On-Orbit Shock Detection during MAG Boom Deployment

The variability from one frangibolt installation to another, the inability to obtain high fidelity ground test data, the long load path from the MAG boom canister to the IMU, and the reduced telemetry rate for the flight sequence all make the tuning the shock detection parameters especially challenging for the MAG boom deployment. Even so, the tuning for GOES-18 nearly achieved the desired performance, as shown in Figure 12. Examination of the lower plot shows that the detection threshold was met for 1 of the 4 gyros, but a shock event will only be identified if 2 of the 4 gyros simultaneously meet the threshold. With this information in hand, the GOES-19 thresholds will once again be adjusted in an attempt to correctly identify the frangibolt initiation of the MAG boom deployment. The GOES-19 shock detection threshold will be lowered to 0.005 rad. As can be seen from the lower plot, there is some risk with this setting that extra shock counts may be recorded as the boom locks up at the end of its deployment at around 80 s.

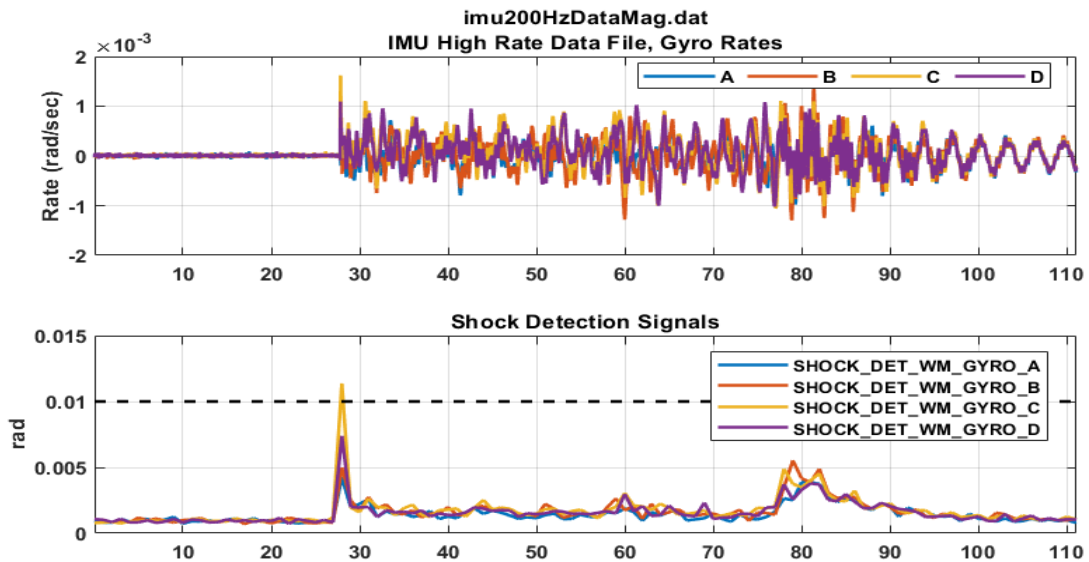


Figure 12. GOES-18 On-Orbit Shock Detection during MAG Boom Frangibolt Release

#### 4 VERIFICATION OF DEPLOYMENT COMPLETION

The shock detection technique discussed above can reliably show the initiation of a deployment activity, but is not capable of verifying the completion of many deployment events. An alternative technique is needed to verify successful deployment completion. For the GOES-R- program a ground-based assessment of the dynamic response has been implemented for various deployment events, two of which are presented in this section. The first of these is the solar array deployment discussed earlier in this paper. There are 10 shock events required to release the solar array from its stowed configuration, which we showed can be reliably detected using the shock detection algorithm. However, shock detection is not reliable for detecting the lockup of the hinge line mechanisms. An alternative approach is presented in this section. The second event presented here is the MAG boom deployment. As discussed above, tuning of the shock parameters proved challenging due to the complex dynamics following the frangibolt release. But these same dynamics can be used to determine whether the collapsible boom has fully deployed and locked into place. As with the onboard shock detection algorithm, high-rate gyro data are available to assess the deployment dynamics. This assessment is not performed onboard, however. A short-duration recording of the high-rate gyro data is downlinked to allow ground-based assessment of each deployment event. Here we present pre-flight gyro rate response predictions and compare with the in-flight gyro rate response for the solar array deployment and for the MAG boom deployment.

##### 4.1 Solar Array Deployment

Once the 4 frangibolts have been fired and 6 SSRDs have been activated, the second stage of the solar array deployment begins. This deployment consists of 2 simultaneous hinge line rotations: the root hinge next to the solar array gimbal rotates 90 deg, and the frame hinge next to the SPP rotates 180 deg. Both of these hinge line rotations must fully complete and lock into place before it is safe to rotate the solar array gimbal. Because the solar array has a significant inertia relative to the bus inertia, the response to the deployment motion is readily observed by the gyros in the IMU. The simulated Z-axis attitude rate response is shown in Figure 13. Because of the hinge line orientation relative to the spacecraft body axes, the responses in the X-axis and Y-axis are small and are not shown. As observed in the plot, there is a fairly large rate response as the motion begins. At ~150 s the root hinge latches into place, followed by the frame hinge at ~170 s. Once both hinges are locked into place, the characteristic resonant frequency of ~0.35 Hz can be easily seen in the rate signature.

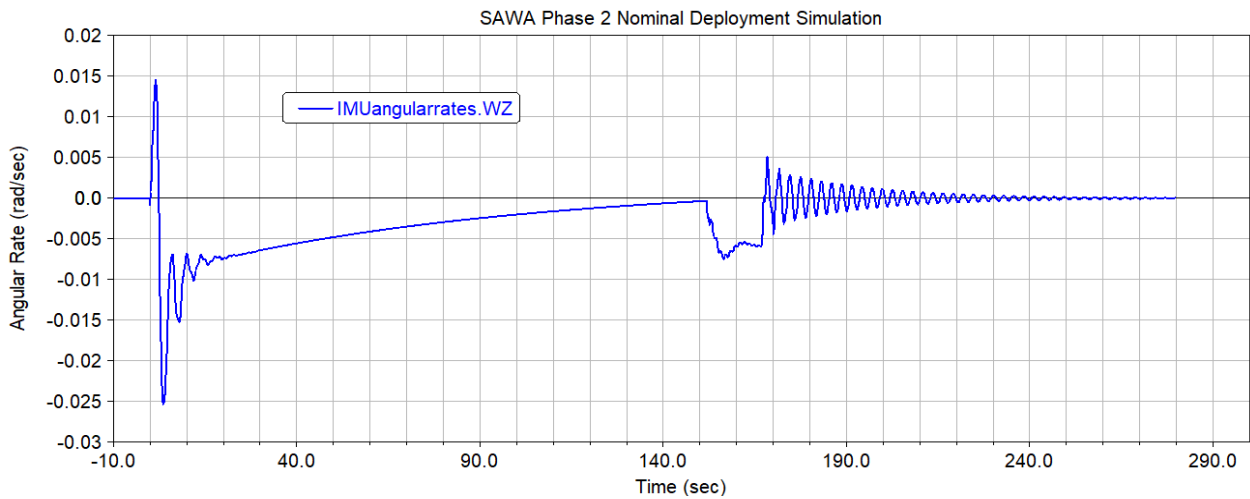


Figure 13. Simulated Solar Array Deployment, Z-axis Attitude Rate

Figure 14 shows the in-flight Z-axis attitude rate responses for both GOES-16 and GOES-17. The initial transient has approximately the same magnitude observed in the simulated response, but the on-orbit behavior appears to have somewhat more damping in the 20 s following the initial transient. The GOES-17 response shows the same behavior as in the simulation, with the root hinge latching first. The GOES-16 response is slightly different, with both the root hinge and the frame hinge latching nearly simultaneously. This variability was not unexpected—either hinge can latch up first depending upon the thermal conditions of the individual hinges and dampers

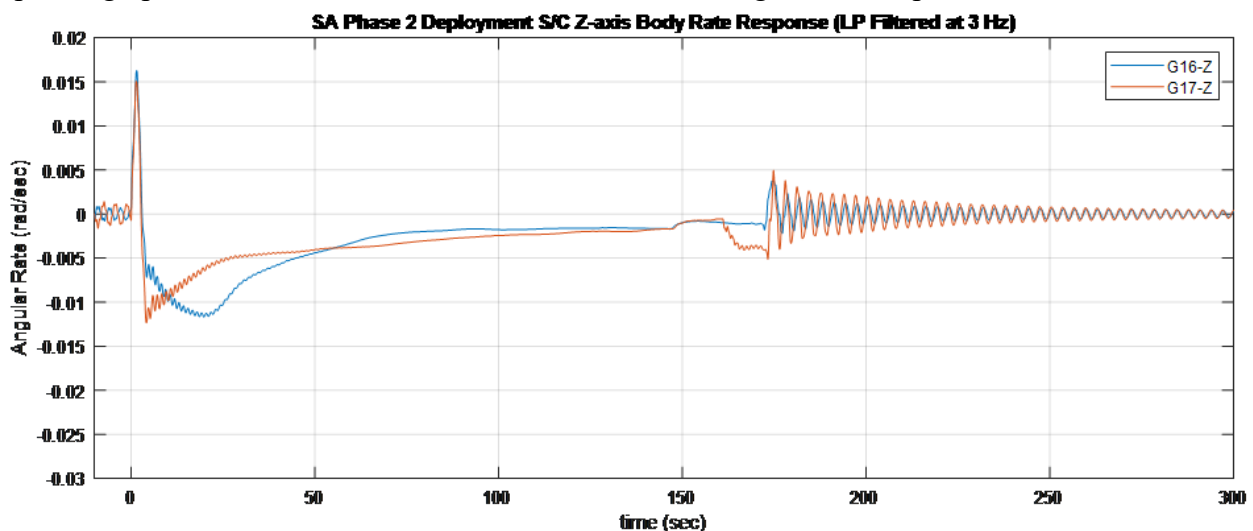


Figure 14. GOES-16 and GOES-17 Solar Array Deployment Flight Results, Z-axis Attitude Rate

The overall deployment time closely matches the simulated response, with the final latch up occurring at ~170 s for both GOES-16 and GOES-17. The deployed frequency following the latch up of both hinge lines is ~0.32 Hz for both vehicles, which is slightly lower than in the simulated response. The simulated deployment used worst-case (high) stiffnesses to ensure that the worst-case loads at lock-up were captured, so the flight frequency was expected to be slightly lower. The observed resonant frequency is consistent with the on-orbit system identification performed later in the on-orbit calibration activities [7]. The characteristic ringing evident in both flight responses indicates a successful deployment, demonstrating that the hinges fully latched in the deployed position.

## 4.2 MAG Instrument Boom Deployment

The 8.5 m collapsible boom has very complex deployment dynamics that are difficult to model accurately. Furthermore, the boom deployment cannot be tested at the spacecraft level, so modeling is based upon component-level demonstrations of the boom deployment. A very simple axial-motion

only boom model was developed to provide representative deployment dynamics, but this model does not accurately capture boom transient motions during unfurling. It does, however, provide a reasonably accurate model of the final deployed resonant frequencies. The deployment results from this model are shown in Figure 15. The frangibolt is fired at 10 s, and the boom is completely unfurled and locked in place 60 s later. The spacecraft attitude rates are considered representative during the boom deployment, but significant variation from this profile was expected to occur during flight. The key observable is the abrupt change in the signature when the boom locks into place.

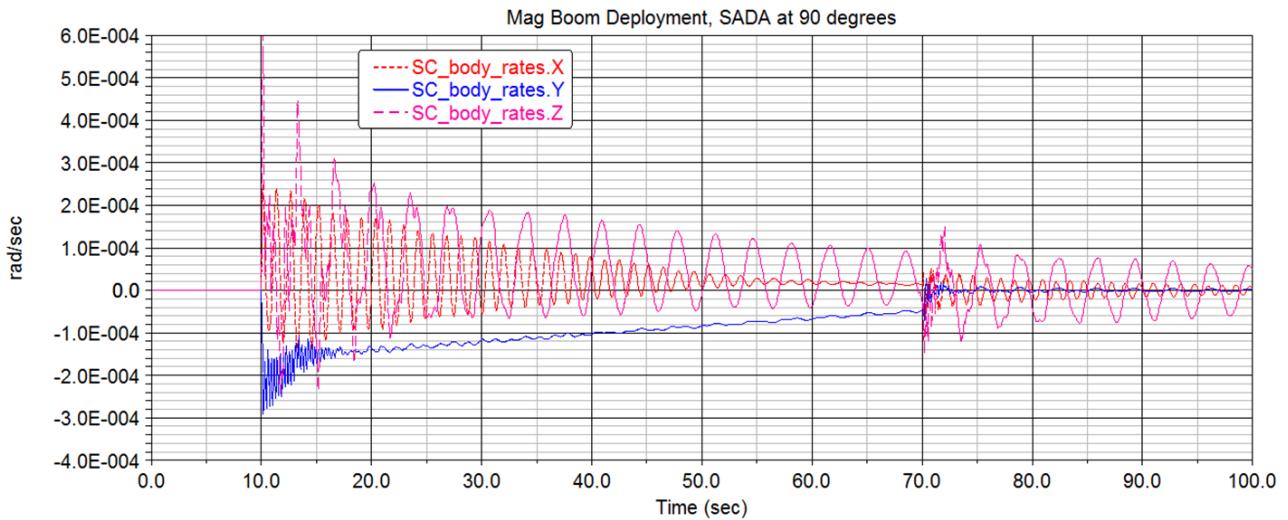


Figure 15. Simulated MAG Boom Deploy Signature

The flight results for the GOES-16 MAG boom deploy are shown in Figure 16. The Y-axis response is shown on the left, and the Z-axis response is shown on the right. The X-axis response is comparatively small and is not shown. As can be seen in the plots, the dynamics following the frangibolt firing at 0 s are more complex than the simulation results, and unlike the simulation, the response is roughly equal in the Y and Z axes.

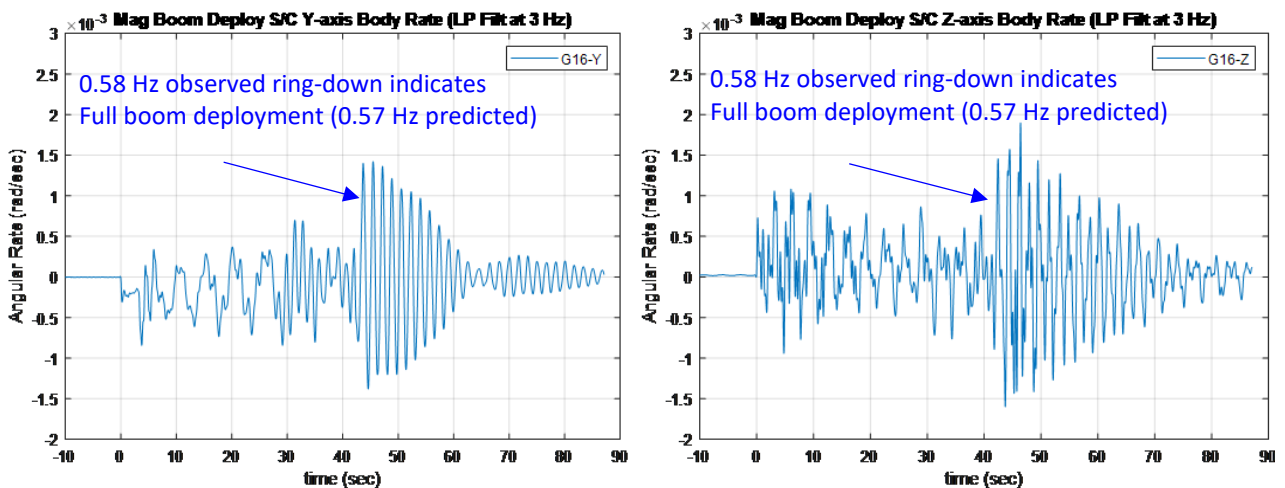


Figure 16. GOES-16 MAG Boom Deploy Flight Results, Y-axis (left) and Z-axis (right)

Rather than sinusoidal responses seen in simulation, the actual response is much more complex as the longerons for each bay sequentially lock into place. Also, the on-orbit attitude rate response is roughly 10X higher than the simulated response. Finally, the observed deployment times of 43 sec and 52 sec for GOES-16 and GOES-17, respectively, are shorter than expected deployment time of 60 sec. Even so, the simulation accurately predicted the resonant frequency of the deployed boom, which was 0.58 Hz as compared with the predicted resonant frequency of 0.57 Hz. The final lockup of the MAG boom is clearly evident in the gyro rate plots, with the expected deployed frequency being observed.

## 5 CONCLUSION

A two-part strategy has been developed by the GOES-R program for verifying appendage deployments. The shock detection algorithm incorporating high-rate gyro data has been successfully deployed operationally, which reliably determines the initiation of deployment events. Development of dynamic models to determine deployment signatures allows verification of deployment event completion. This has also been deployed operationally. The two-part strategy utilizes existing spacecraft resources without the addition of deployment sensors, and has been shown to be compatible with low-rate telemetry. In this paper, we have presented both simulation results and flight results for representative deployment events across multiple vehicles. Guidelines have been provided for which events the shock detection algorithm can easily be applied. An example deployment with complex dynamics was included where the parameter tuning was more challenging. Nonetheless, the parameters can be tuned such that the deployment initiation is readily observed in telemetry even for deployments with complex dynamics.

## 6 ACKNOWLEDGEMENTS

This work was performed at Lockheed Martin Space, under NASA contract NNG09HR00C, and at the National Aeronautics and Space Administration Goddard Space Flight Center. The authors gratefully acknowledge the many individuals who have contributed in various ways through GOES-R program workshops and reviews, and have helped develop improved tools and techniques used by the development team and the operations team. Special thanks are extended to Derrick Early at Chesapeake Aerospace for his expert technical review of this manuscript and for his insightful feedback. The deployment verifications presented in this paper have enabled the successful transition to operational status of three GOES-R program vehicles.

## 7 REFERENCES

- [1] T. J. Schmit, Jun Li, Jinlong Li, W. F. Feltz, J. J. Gurka, M. D. Goldberg, K. J. Schrab, “The GOES-R Advanced Base-line Imager and the Continuation of Current Sounder Products,” *Journal of Applied Meteorology and Climatology*, 47, 2696–2711, 2008.
- [2] J. Chapel, D. Stancliffe, T. Bevacqua, S. Winkler, B. Clapp, T. Rood, D. Gaylor, D. Freesland, A. Krimchansky, “Guidance, Navigation, and Control Performance for the GOES-R Spacecraft,” *Proceedings of the 9th International ESA Conference on Guidance, Navigation & Control Systems*, Oporto, Portugal, Jun 2014.
- [3] J. Chapel, D. Stancliffe, T. Bevacqua, S. Winkler, B. Clapp, T. Rood, D. Gaylor, D. Freesland, A. Krimchansky, “Guidance, Navigation, and Control Performance for the GOES-R Spacecraft,” *CEAS Space Journal*, DOI 10.1007/s12567-015-0077-1, March 2015.
- [4] J. Chapel, D. Stancliffe, T. Bevacqua, S. Winkler, B. Clapp, T. Rood, D. Freesland, A. Reth, D. Early, T. Walsh, A. Krimchansky, “In-Flight Guidance, Navigation, and Control Performance Results for the GOES-16 Spacecraft,” *Proceedings, 10th International ESA Conference on Guidance, Navigation & Control Systems*, Salzburg, Austria, May 2017.
- [5] D. Freesland, D. Carter, J. Chapel, B. Clapp, J. Howat, and A. Krimchansky, “GOES-R Dual Isolation,” *Proceedings, 2015 AAS Guidance and Control Conference*, Breckenridge, CO, Feb 2015.
- [6] D. Carter, B. Clapp, D. Early, D. Freesland, J. Chapel, R. Bailey, A. Krimchansky, “GOES-16 On-Orbit Dual Isolation Performance Characterization Results,” *Proceedings of 10th International ESA Conference on Guidance, Navigation & Control Systems*, Salzburg, Austria, Jun 2017.
- [7] J. Chapel, T. Bevacqua, D. Stancliffe, G. Ramsey, T. Rood, D. Freesland, J. Fiorello, A. Krimchansky, “GOES-R Spacecraft Verification and Validation Compared with Flight Results,” *Proceedings of the 2019 AAS Guidance and Control Conference*, Breckenridge, CO, Feb 2019.